Received: 7 October 2022 | Accepted: 17 November 2022

DOI: 10.1002/pamm.202200166

Experimental investigation of carbon long fiber reinforced polyamide 6 exposed to environmental conditions

Nicolas Christ[1,3,*], **John Montesano**[2], and **Jörg Hohe**[3]

[1] Institute for Applied Materials, Karlsruhe Institute of Technology, Straße am Forum 7, 76131 Karlsruhe, Germany

[2] Department of Mechanical and Mechatronics Engineering, University of Waterloo, 200 University Ave W, Waterloo, Ontario, Canada

[3] Fraunhofer Institute for Mechanics of Materials IWM, Wöhlerstrasse 11, 79108 Freiburg, Germany

To enhance the possibilities in lightweight constructions in terms of processability and recyclability, fiber reinforced thermoplastics are a promising class of materials. In this context, the fiber-matrix interface has a major influence on the mechanical properties of the composite. With polyamide 6 (PA6) being a hygroscopic thermoplastic, the effects of elevated humidity and temperature on the mechanical behavior must be considered [1]. This study aims to characterize the micro-mechanical material properties of carbon long fiber reinforced PA6 in quasi-static tensile tests after exposure to elevated temperature and humidity levels. Therefore, the specimens are conditioned in different climates and tested afterwards. In order to determine the initiation and propagation of matrix cracks, interface failure, and fiber fracture, the experiments are conducted on a micro-scale with an average cross-section of 0.03 mm^2. The damage patterns are captured using optical microscopy and SEM images. The effects of conditioning at various temperature and humidity levels are discussed. The main results are the qualitative description of the degradation of mechanical properties due to hydrothermal effects.

1 Introduction

In the field of lightweight construction, fiber reinforced polymers (FRP) established an ever increasing market value, due to their high specific strength and stiffness properties [2]. The need for more environmentally sustainable materials and the demand to design complex components with this class of materials motivates the use of long fiber reinforced thermoplastics. The reason for this is that thermoplastics, due to their molecular structure, can be remelted and are therefore optimal materials for a sustainable recycling process. This is a decisive difference to conventionally used polymers, such as thermosets, as these irreversibly disintegrate when the decomposition temperature is exceeded after curing.

Although they have the highest possible stiffness and strength values within the FRP class, continuous reinforcing fibers only allow limited design freedom. Especially in cases of double-curved surfaces, wrinkling occurs, which requires a special assessment. In contrast, discontinuous reinforcing fibers allow for a much greater freedom of design and can be manufactured in easily automated processes, such as injection molding or extrusion. This is achieved while still maintaining relatively high specific stiffness and strength properties, especially in the case of long fiber reinforced polymers (LFRP).

In order to gain a deeper understanding of LFRP, it is paramount to investigate the behavior of each constituent and the composite itself. [3] has shown the influence of the interface mechanics on the performance of the whole composite. By studying the experimental results and numerical modeling, it was shown that the knowledge of the interface parameters is important to determine the fracture behavior of the composite in advance. Through the numerical investigation with different parameters, such as interfacial shear strength and fracture energy, it was shown that different sets of parameters lead to different failure behaviors. Consequently, this motivates the qualitative investigation of the fracture behavior in order to reproduce it in subsequent numerical simulation and thus to find robust parameters. A suitable scale to gain more insight into the stress transfer effects from fiber to matrix and into damage mechanisms in and around the interface is the micro-scale. On this scale, individual fibers can be distinguished and crack initiation and propagation is observable in detail. However, a challenge at the microscale is that the microstructure varies greatly from sample to sample, making statistical analysis difficult.

Due to their polarity between macro-chains, some thermoplastics, e.g. the here investigated PA6, are prone to water absorption and thereby are considered hygroscopic materials (cf. [4]). In [5] and [6] it was shown how water and temperature affect the mechanical properties of carbon fiber reinforced PA6. Their conclusive findings are that the absorption of water reduces both stiffness and strength of the composite. Along with the nature of thermoplastic materials of showing pronounced viscous behavior even at lower temperatures, e.g. room temperature, it is important to consider both humidity and temperature effects on the mechanical propeties.

* Corresponding author: e-mail nicolas.christ@kit.edu, phone +49 761 5142-551

2 Methodology

The material of interest is a discontinuously, long carbon fiber reinforced PA6. To produce microscopic samples, $400 \times 400 \times 3$ mm^3 plates were manufactured in a LFT-D process at the Fraunhofer ICT, Germany. The process consists of two counter-rotating twin extruders. The first extruder melts the PA6 granules and feeds the melt into the second extruder with a steady addition of continuous carbon fibers. Within the second extruder, the continuous fiber is broken into smaller sections by the applied shear forces. The second extruder finally outputs a plastificate, which is transferred to a press and pressed into sheets of given dimensions. The resulting fiber length distribution was subsequently determined by means of a burn-off process for a single plate. The median fiber length was found to be 2.94 mm, while the average fiber length was 4.35 mm with a standard deviation of 4.07 mm. The longest fiber had a length of 19.33 mm.

The plate was divided into a charge and flow area, for which the latter is expected to provide a more uniformly aligned fiber orientation in flow direction (cf. Fig. 1). From the flow area, microscopic samples were manufactured with an average cross-sectional area of 0.03 mm^2 at its most narrow width, which are also depicted in Fig. 1. The specimens were ground and polished under a diamond suspension. One such sample is depicted in Fig. 2. To investigate the effects of elevated temperature and humidity exposure, $n = 5$ samples were immersed in distilled water at 70 °C for 80 hours. The remaining $n = 5$ samples were conditioned at room temperature and humidity.

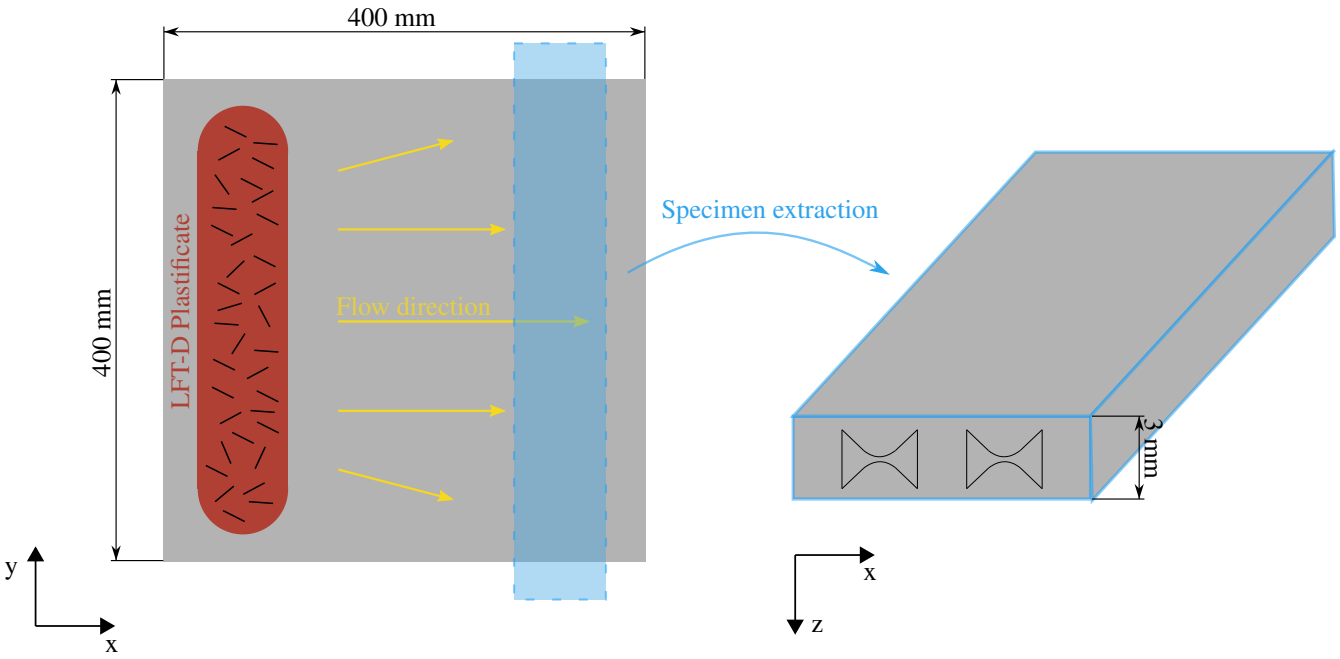

Fig. 1: LFT-D plates divided into charge area (where the plastificate is positioned) and flow area on the right side of the plate. Specimens were extracted from the flow area within the x-z-plane.

Following the conditioning, the specimens were investigated with a light microscope and SEM to optically evaluate possible degradation effects. Afterwards, they were tested in a micro-mechanical quasi-static tension setup at room temperature (23 °C) and a relative humidity of 45 %. The displacement rate between the clamps was set to $\dot{u} = 3{\cdot}10^{-4}$ mm/s, which corresponds to an average strain rate of $\dot{\varepsilon} = 1$ %/min, following ISO 527-1. Following the evaluation of mechanical properties, i.e. stiffness, strength and elongation at failure, the fracture surfaces were investigated by SEM analysis once more.

3 Results and discussion

3.1 Optical assessment before testing

The optical SEM assesment of the specimen after immersion in distilled water at an elevated temperature reveal a pronounced crack formation in the matrix surface, as can be seen in Fig. 3. The cracks appear to be propagating between interfaces with no preferred direction, indicating a volumetric effect. Interface degradation near the surface, i.e. separation of fiber and matrix, is visible.

The interpretation of these findings is that water diffusion into the hygroscopic matrix material is accelerated at elevated temperatures (cf. [7]), resulting in swelling of the polymer (cf. [4]). The swelling is associated with compressive stresses that rapidly dissipate in the viscous matrix material at elevated temperatures. Once the sample is removed from the oven, the large temperature gradient causes heat to flow out of the material, resulting in an opposite contraction of the polymer due to the increased coefficient of thermal expansion compared to the fiber. The stiffer fibers behave like a contraction inhibitor,

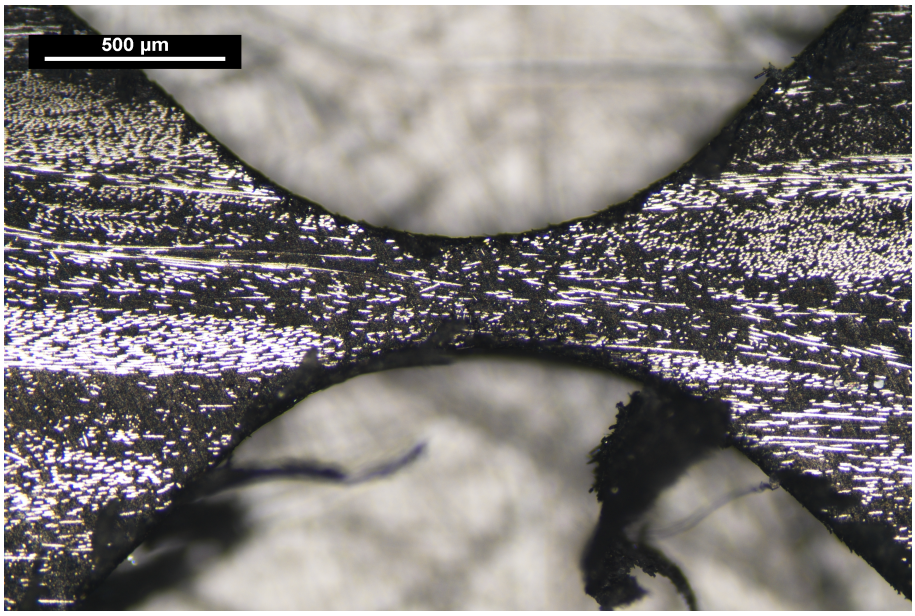

Fig. 2: Light microscope image of a specimen after polishing.

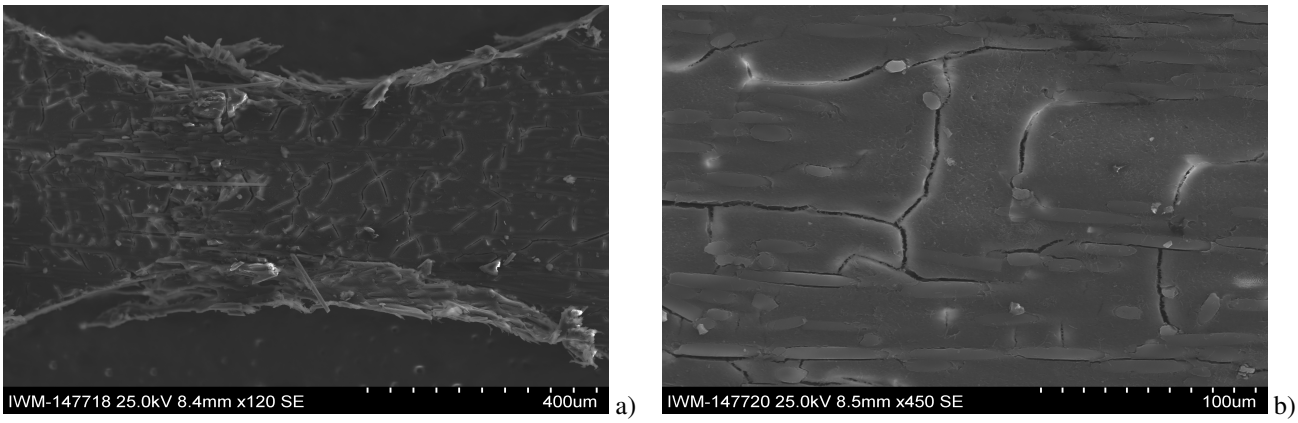

Fig. 3: SEM image of specimen after immersion in distilled water at 70 °C for 80 hours. Whole specimen with a magnification of x120 in **a**, detailed view of the same specimen at x450 in **b**.

inducing a volumetric tensile stress state within the polymer, which explains the formation of cracks around and between the fiber interfaces.

To investigate the progressive cracking, another series of tests was started at reduced temperature. Here, the specimens were stored in 50 °C water and examined with the SEM at different times. The investigation of a single specimen is depicted in Fig. 4. It is confirmed that the cracking propagates over time. In contrast to the higher temperature of 70 °C, the cracks are finer and do not penetrate as deeply into the material. Most likely, this is a swelling and shrinking process expressed by the fibers protruding further from the polymer surface as time progresses. Again, interfacial separation can be observed near the surface. The reduced cracking is likely due to the lower temperature causing a lower temperature gradient when the specimens are removed from the oven, supporting the above hypothesis and suggesting that temperature and humidity both affect the degradation mutually.

3.2 Mechanical testing

The results for the quasi-static testing are displayed in Fig. 5. Generally, a large scatter in the results was observed, which can be explained by the geometric properties of the specimens. Due to the small cross-sectional area of 0.03 mm^2, the heterogeneous micro-structure does not average over the specimen's volume, i.e. one sample may contain fiber-rich regions whereas another does not. Additionally, fiber distribution and content were found to vary significantly between samples.

The statistical evaluation can be seen in Fig. 6. No difference in stiffness properties was observed between dry and wet specimens, which is in contrast to findings in [7], [8] and [1]. So far, this contradiction lacks a reliable explanation, but a size effect is likely. One hypothesis is that all specimens, including the ones that were not immersed in water (called dry

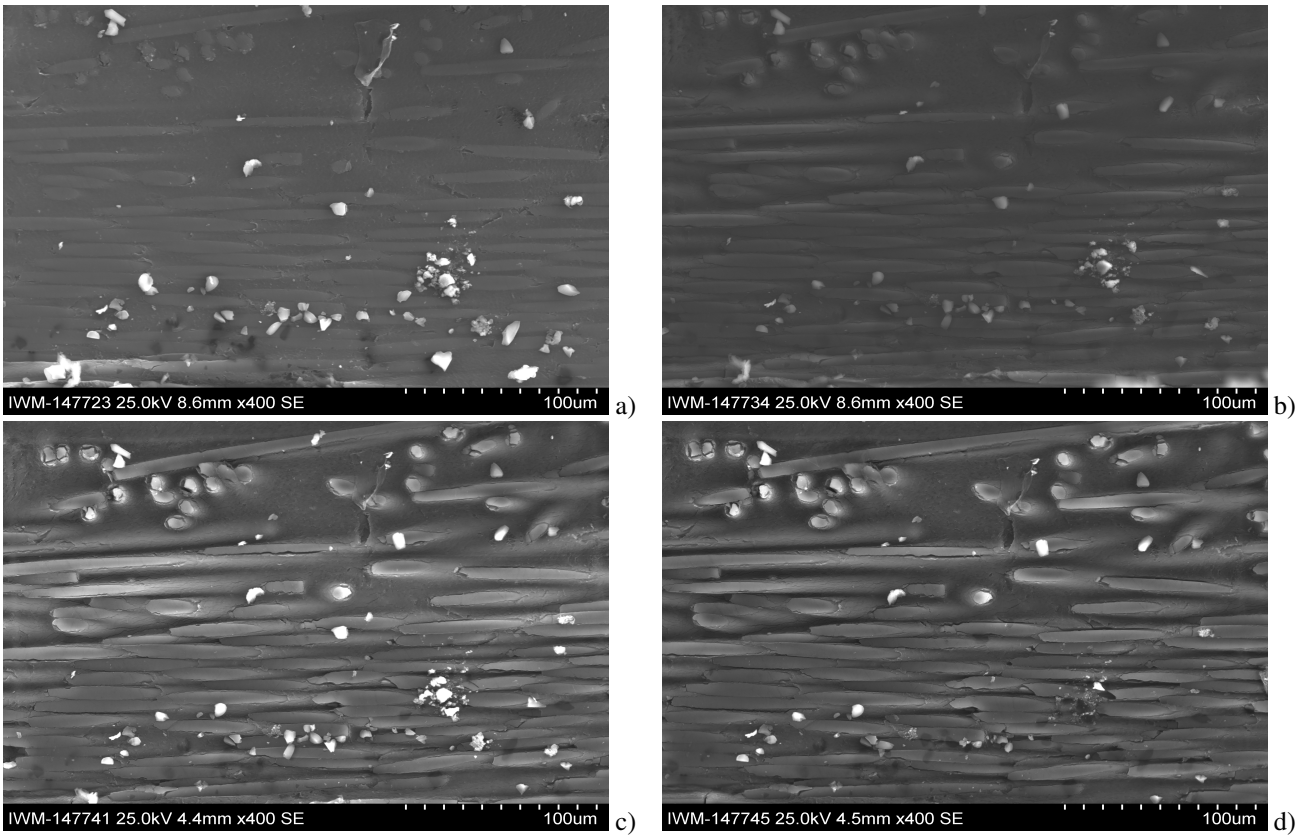

Fig. 4: SEM image of specimen after immersion in distilled water at 50 °C. Specimen after 0 hours in **a**, 22 hours in **b**, 62 hours in **c** and 132 hours in **d**.

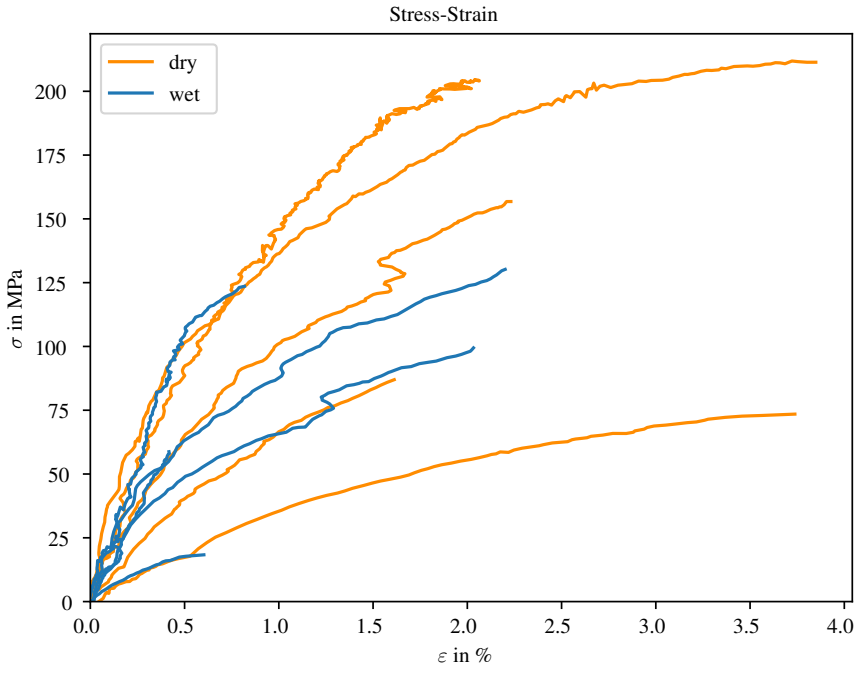

Fig. 5: Stress-Strain curve for dry and wet specimens.

specimens), came in contact with water during the specimen extraction. It is possible that the conditioning environment (23 °C, 45 % r.H.) and conditioning time for the dry samples were not sufficient for the absorbed water to diffuse out of the

specimens again. It must be mentioned here that the small number of samples combined with a highly varying microstructure makes statistical analysis less meaningful. This must be taken into account when interpreting the results.

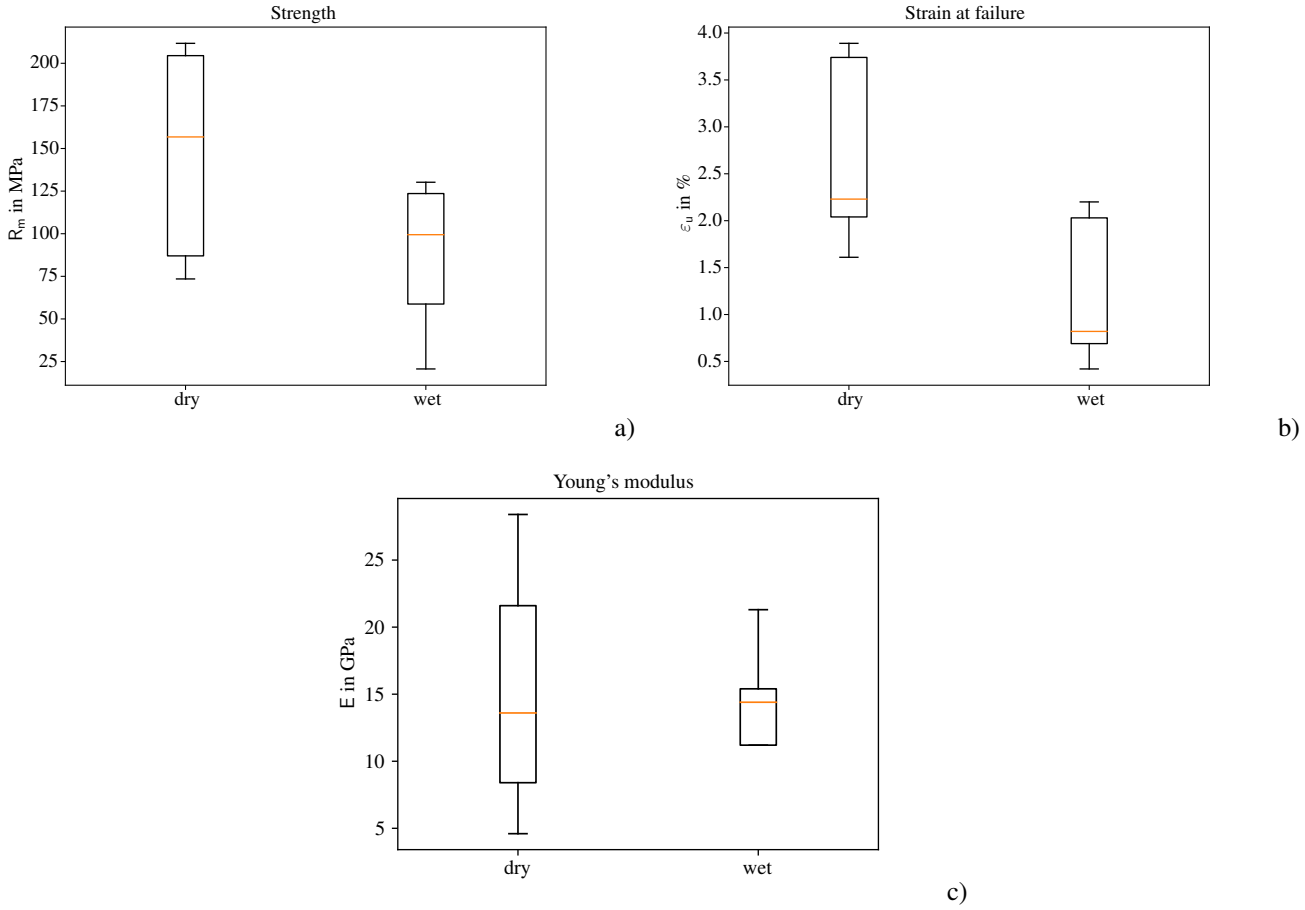

Fig. 6: Box plot comparing mechanical properties of dry and wet specimens: **a**) strength, **b**) strain at failure, **c**) Young's modulus.

The strength and elongation at failure are significantly reduced for the wet specimens. Since significant crack formation was observed after the treatment at elevated temperature and humidity, the effective cross-section is reduced and stress concentration lead to a quicker propagation of crack surfaces and thereby to the observed accelerated failure.

3.3 Optical assessment after testing

After failure, SEM images of the fracture surfaces of dry and wet specimens were investigated. In Figs. 7 and 8, it can be seen in both wet and dry specimens that the matrix clearly fringes in the fracture surface. In combination with the image sequence of the tests, in which a continuous crack growth, large local strains and a pronounced necking were observed in contrast to an instantaneous brittle fracture with limited deformation, ductile matrix failure is confirmed as the dominant fracture mechanism within the polymer.

Additionally, both wet and dry specimens show blank fibers free of matrix residues, indicating a weak interface at which the crack propagated. Especially for the wet specimens, it is visible that the fibers adjacent to the surface debonded completely, indicating a weakening moisture effect on the interface (cf. Fig. 7 **a**).

Fiber-rich regions appear to be circumscribed by cracking, which is due to the jump in stiffness properties between a matrix-rich and fiber-rich area. In conclusion, the predominant fracture patterns are ductile matrix cracks and fiber pullouts, suggesting that the interfaces of the dry specimens were also damaged during processing or that the bond was weak to begin with.

3.4 Conclusion

Discontinuously, long carbon fiber reinforced PA6 was examined at the micro-scale to explore the effects of hydrothermal aging. $n = 5$ specimens were stored in distilled water at 70 °C for 80 hours (wet specimens), while $n = 5$ specimens were conditioned at 23 °C and 45 % relative humidity (dry specimens). After 80 hours, the wet specimens showed significant formation of cracks with visible damage at the fiber-matrix interface. The crack initiation and propagation was explained

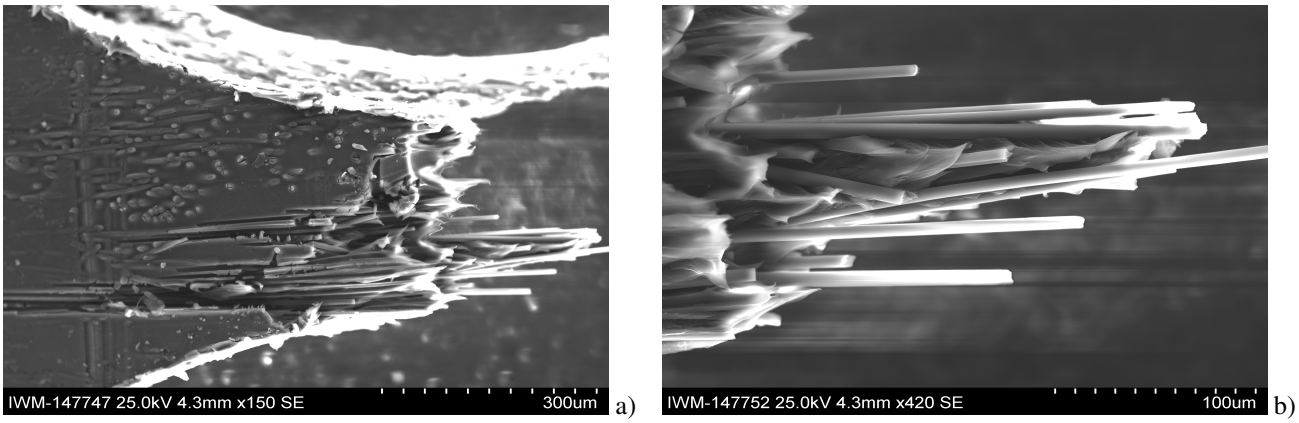

Fig. 7: SEM image of fracture surface of wet specimen after immersion in distilled water at 70 °C for 80 hours. Left fracture surface with a magnification of x150 in **a**, detailed view of the same specimen at x420 in **b**.

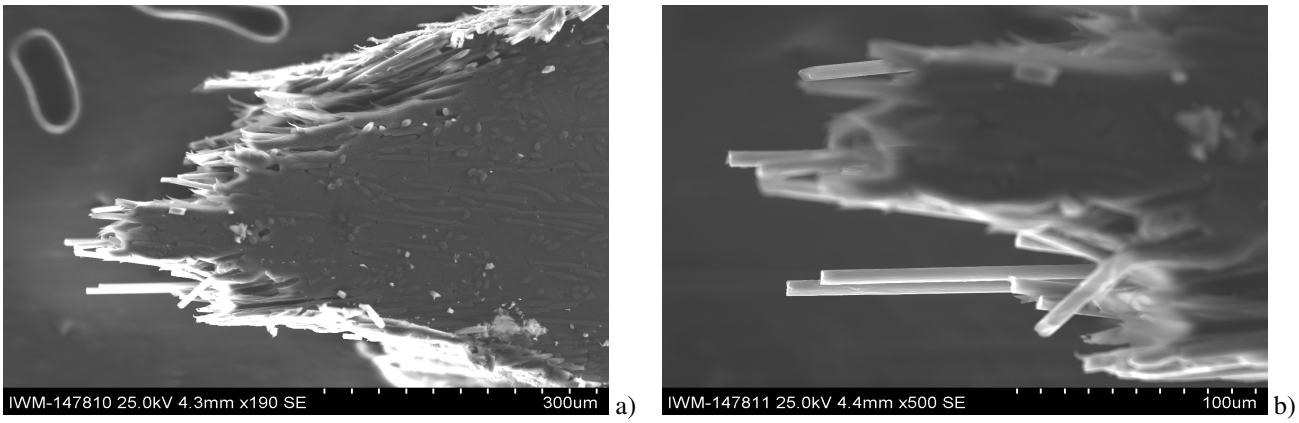

Fig. 8: SEM image of fracture surface of dry specimen. Right fracture surface with a magnification of x190 in **a**, detailed view of the same specimen at x500 in **b**.

by a swelling-contraction effect due to different thermal expansion coefficients between fiber and matrix. In the quasi-static tensile test, the wet specimens exhibited significantly lower tensile strength and elongation at break, while the modulus was indifferent to that of the dry specimens. The hypothesis is that the modulus of the dry specimens also deteriorated due to water contact during manufacturing. The predominant failure for both types of conditioning was found to be ductile matrix fracture and fiber pull-out, indicating a weak fiber-matrix bonding.

Acknowledgements The research documented in this proceeding has been funded by the Deutsche Forschungsgemeinschaft (DFG, German Research Foundation), project number 255730231, within the International Research Training Group "Integrated engineering of continuous-discontinuous long fiber reinforced polymer structures" (GRK 2078). The support by the German Research Foundation (DFG) is gratefully acknowledged. Open access funding enabled and organized by Projekt DEAL.

References

[1] L. Sang, Y. Wang, C. Wang, X. Peng, W. Hou, L. Tong, Moisture diffusion and damage characteristics of carbon fabric reinforced polyamide 6 laminates under hydrothermal aging, Composites Part A: Applied Science and Manufacturing 123 (2019) 242–252. doi:10.1016/j.compositesa.2019.05.023.

[2] S. Pimenta, S. T. Pinho, Recycling carbon fibre reinforced polymers for structural applications: technology review and market outlook, Waste management (New York, N.Y.) 31 (2) (2011) 378–392. doi:10.1016/j.wasman.2010.09.019.

[3] M. Schober, On the characterization and modeling of interfaces in fiber reinforced polymer structures. doi:10.5445/IR/1000100455.

[4] L. Monson, M. Braunwarth, C. W. Extrand, Moisture absorption by various polyamides and their associated dimensional changes, Journal of Applied Polymer Science 107 (1) (2008) 355–363. doi:10.1002/app.27057.

[5] L. Sang, C. Wang, Y. Wang, W. Hou, Effects of hydrothermal aging on moisture absorption and property prediction of short carbon fiber reinforced polyamide 6 composites, Composites Part B: Engineering 153 (2018) 306–314. doi:10.1016/j.compositesb.2018.08.138.

[6] H. Piao, L. Chen, Y. Kiryu, I. Ohsawa, J. Takahashi, Influence of water absorption and temperature on the mechanical properties of discontinuous carbon fiber reinforced polyamide 6, Fibers and Polymers 20 (3) (2019) 611–619. doi:10.1007/s12221-019-8767-5.

[7] L. Silva, S. Tognana, W. Salgueiro, Study of the water absorption and its influence on the young's modulus in a commercial polyamide, Polymer Testing 32 (1) (2013) 158–164. doi:10.1016/j.polymertesting.2012.10.003.

[8] H. Piao, Y. Kiryu, L. Chen, S. Yamashita, I. Ohsawa, J. Takahashi, Influence of water absorption on the mechanical properties of discontinuous carbon fiber reinforced polyamide 6, Journal of Polymer Research 26 (3) (2019). doi:10.1007/s10965-019-1695-7.